



25<sup>th</sup> ABCM International Congress of Mechanical Engineering  
October 20-25, 2019, Uberlândia, MG, Brazil

## COB-2019-0130 FAILURE DETECTION IN GEAR TEST RIG

**Rodrigo Metzger da Silva<sup>1</sup>**

**Lucas Barreiros Robatto<sup>2</sup>**

**Ronnie Rodrigo Rego<sup>3</sup>**

Instituto Tecnológico de Aeronáutica – ITA/CCM

Praça Marechal Eduardo Gomes, 50

12228-900 – São José dos Campos - SP

<sup>1</sup>metzger@ita.br, <sup>2</sup>robatto@ita.br, <sup>3</sup>ronnie@ita.br

**Abstract.** *The detection of failure in its first stages provides a significant assistance in the maintenance schedule of the equipment and allows the avoidance of unpredicted stops. The failure analysis has an important role in the recognition of an equipment standard behavior and in the identification of failures during operation. Using a gear test rig, a failure analysis method based on vibration techniques was developed in the present study. Through accelerometers, the vibration signals were acquired during a gear durability test. After seven hours of test, a bearing failure occurred and it provided the database for this research. It was possible to detect frequency of vibration with rising amplitude due to bearing failure on the acquired signal. The failure and the acquired data presented a coherent relation by the application of the developed method. The resulting procedure can then be adopted in other studies and in the failure detection in test rigs and real application machines.*

**Keywords:** *failure detection, maintenance, vibration techniques, bearing failure, gear test rig*

### 1. INTRODUCTION

The development of new methods and materials for machine elements manufacturing is associated with the need to evaluate the durability of these components. Monitoring the behavior and identifying the failures of an equipment in its initial stages reflect in scheduled stops and in avoidance of non-predicted failures, allowing higher productivity and costs reduction.

The failure analysis and diagnosis of rotary machines can be used for the development of predictive methods based on the behavior data from the equipment during operation. There are three basic steps to predict the failure of a machine: to define the standard behavior of the equipment, to find the root cause of the previous failures and to predict the occurrence of these failures (Liu et al., 2018).

Bearings are between the most common elements in a rotary machine. Although these are designed to a high level of durability, bearing failures are frequent causes of machine stops. Monitoring this element behavior guarantees the detection of early stages of the failure, providing enough time for maintenance and avoiding catastrophic stops in the equipment (Dybala, 2018).

Among other methods of monitoring the component life, those based on vibration are very reliable and widespread methods. However, vibration signals contain a high presence of noise, especially in rotary machines. Therefore, the useful information of the signal should be filtered during the analysis (Hoang and Kang, 2018).

The present study uses a gear test rig as a tool to perform the failure analysis of the components which failed during a gear durability test. During one of the experiments, a bearing failed due to contact fatigue. The development of a failure detection method was then performed using the acquired vibration signal from the test, and the corresponding results are here described.

### 2. MATERIALS AND METHODS

The materials and methods section is divided in four subsections: the equipment where the tests were performed, evaluation of the bearing failure, deterministic frequencies and signal analysis.

#### 2.1 Gear test rig

In order to generate the failure, an equipment that could induce the damage and guarantee the running parameters control was necessary. The gear test rig where the tests were performed is based on the back-to-back concept, which

allows the optimization of the load application (Aslantas et al., 2004). It was developed to perform tests with gears at two distinct center distances, allowing a high range of gear ratio. Figure 1 shows the gear test rig.

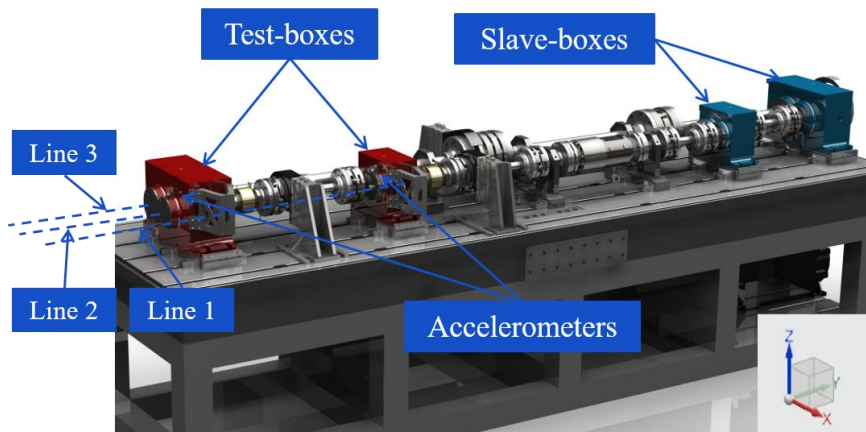


Figure 1. Gear test rig concept of the study

The test gear and the bearings of this study are located inside one of the test-boxes. The bearing was located close to the driven gear on the gearbox. The slave-boxes have the same gear ratio of the test-boxes and they have the main purpose of transmitting the torque and the speed to close the power loop.

The load application on the test rig can be performed manually or by a hydraulic torsion motor controlled by software. In the case of the study, torque was applied manually. An electric motor provides the rotational speed and a thermoregulator unit controls the temperature and the level of lubricant inside the test-box. These four parameters, speed, torque, temperature and lubricant level are the main responsible for the gear performance during the test (FZG, 1992). Transducers located in each line of the rig perform the torque monitoring.

Each test-box was assembled with three uniaxial accelerometers for vibration monitoring, each mounted on an orientation axis, X, Y and Z. They were located in the front cover of the gearbox, right on top of the tested gear shaft. Figure 2 presents the accelerometers mounted.

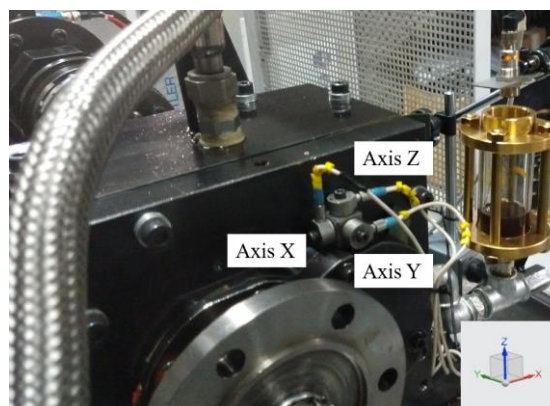


Figure 2. Accelerometers mounted on the Test-box

The accelerometers model was an Endevco® 7251A-500, with a frequency range of 2 Hz to 10 kHz. The bearing failure occurred during one of the gear durability tests, seven hours after the test had started. The parameters of the test are shown in Table 1.

Table 1. Parameters during the test

Parameters	Value
Number of teeth on test drive gear [-]	31
Number of teeth on driven gear [-]	37
Rotation on line 1 shaft [rpm]	3500
Applied torque on line 1 [N.m]	210
Temperature on test-box [°C]	90

## 2.2 Bearing failures

While running, some micro-slips occur on the contact faces of the bearings. This occurs mostly due to distinct elastic properties of the contact surfaces and the different radius of curvature between them. This combination of rolling and sliding potentiates the contact fatigue failure, promoting the crack formation in the subsurface of the contact area (Campanha, 2008).

After the formation, the crack propagates until the material removal occurs. This material removal from the surface characterizes the condition of contact fatigue failure in bearings. Figure 3 shows the inner race of the bearing on the shaft of line 1 of the test rig.



Figure 3. Inner race bearing failure observed after inspection

In the damage area, it was possible to identify the surface cracks, characterizing the failure as contact fatigue.

## 2.3 Deterministic frequencies

Bearing defects can excite vibrations on the contact surfaces around them. This effect can be verified by monitoring the behavior of the bearing through vibration measurements (Brito et al., 2011). To identify the bearing fundamental frequencies, the Eq. (1) to (4) are presented by Graney and Starry (2012), where  $N(-)$  is the number of spheres on the bearing,  $F(\text{Hz})$  the rotation frequency of the shaft,  $B(\text{m})$  represent the sphere diameter,  $P(\text{m})$  the primitive diameter of the sphere and  $\theta(^{\circ})$  is the contact angle of the bearing. Through these frequencies it is possible to correlate the bearing fundamental frequencies with the fault frequencies that can appear in the bearing.

$$F_{inner\ race}(\text{Hz}) = \frac{N}{2} \times F \times \left(1 + \frac{B}{P} \times \cos \theta\right) \quad (1)$$

$$F_{outer\ race}(\text{Hz}) = \frac{N}{2} \times F \times \left(1 - \frac{B}{P} \times \cos \theta\right) \quad (2)$$

$$F_{fundamental\ train}(\text{Hz}) = \frac{F}{2} \times \left(1 - \frac{B}{P} \times \cos \theta\right) \quad (3)$$

$$F_{ball\ pass}(\text{Hz}) = \frac{P}{2B} \times F \times \left[1 - \left(\frac{B}{P} \times \cos \theta\right)^2\right] \quad (4)$$

The geometric characteristics of the four-point bearing, QJ 206 MPA from NKE that was used during the test are presented on Table 2.

Table 2. Bearing characteristics (NKE, 2012)

Parameters	Name code	Value
Number of balls [-]	$N$	12
Shaft frequency [Hz]	$F$	58,33
Ball diameter [m]	$B$	$9,525 \times 10^{-3}$
Pitch diameter [m]	$P$	0,046
Contact angle [ $^{\circ}$ ]	$\theta$	35

## 2.4 Signal analysis

Identifying a non-standard signal or a malfunction in the system, may indicate the beginning of a fault. For this purpose, the standard behavior should be firstly established, which represents a normal functioning of the component. It is possible then to use it as a basis of comparison for the new observed condition (Kotu, 2015).

According to Mohammed et al. (2013), statistical methods are used to obtain a signal or a function that describes the behavior of the analyzed system in order to evaluate or predict a failure condition. In the study developed by Wu et al. (2008), the methods RMS (root mean square) and Kurtosis were those that presented the best performance for this purpose.

The RMS analysis assists the determination of a mean amplitude of a variable signal. Also known as effective value, RMS corresponds to the mean value of a signal if it is continuous. The calculation consists of taking the square root of the sum of squares mean of a data package.

In order to better understand the vibration signal, analysis methods are used to make the visualization easier. The frequency analysis is the most common method and uses the FFT (Fast Fourier Transform) to convert the signal from the time domain to the frequency domain. The frequency domain makes it easier to visualize the vibration phenomena, characterized by a periodic behavior. Thus, the signal that was distributed over time is condensed into a single point, referring to its operational frequency.

The waterfall analysis is a method that uses the frequency domain to evaluate a change of state. This method consists of capturing a set of data in the time domain, transforming it to the frequency domain and plotting this set side by side to sets from other moments in time.

## 3. RESULTS AND DISCUSSION

The first evidence of the failure occurred due to the presence of a non-characteristic sound noise during the execution of the gear durability test. In an attempt to identify the noise source, the test was temporarily paused for inspection in the test-box and the bearing failure was identified.

The vibration signal analysis of the gearbox where the bearing was mounted also gave indications of the occurrence of the failure. Figure 4 shows the data from the last hour of the test and the moment when the failure became noticeable through the signal inspection in time domain on axis Y direction.

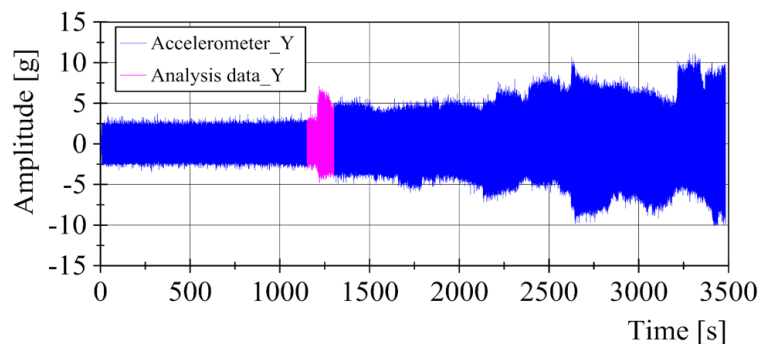


Figure 4. Vibration signal from the last hour of test

The highlighted region on Figure 4 represents the moment when the vibration behavior changed. It was considered that the data before the highlighted region represents a standard behavior of operation. From then on, a disturbance is noted and is characterized by the increase and variation of the amplitude of the vibration signal, which indicates the occurrence of the failure.

Table 3 shows the values obtained from the RMS analysis of the time vibration signal. The values correspond to the RMS mean of an interval of 60 seconds before and after the failure occurrence. The standard deviations of these values were also calculated. It was possible to identify the Y-axis as the direction with more increase of vibration amplitude.

Table 3. RMS analysis from the time domain signal

Direction	Before failure		After failure	
	RMS [g]	Stand. Deviation[g]	RMS [g]	Stand. Deviation[g]
X Axis	0,771	0,042	0,962	0,058
Y Axis	0,610	0,037	1,000	0,054
Z Axis	0,956	0,057	1,131	0,064

With the failure revealed on the inner race of the bearing, the characteristics presented on Table 2 were introduced on Eq. 1 to 4 and it was possible to identify the bearing fundamental frequencies. For the inner race of the bearing used on the test the frequency was 409,37 Hz. For the outer race, fundamental train and ball pass it was 291 Hz, 21 Hz and 137 Hz respectively.

A waterfall analysis was carried out with the data from the highlighted section on Figure 4. This section was selected because it represents the moment of transition between a standard behavior to the beginning of the disturbance on the system. For the waterfall analysis, Fast Fourier Transforms were performed at each half of a second in a range of 150 seconds. The results are shown in Figure 5 with the frequency axis highlighted only on the area of interest

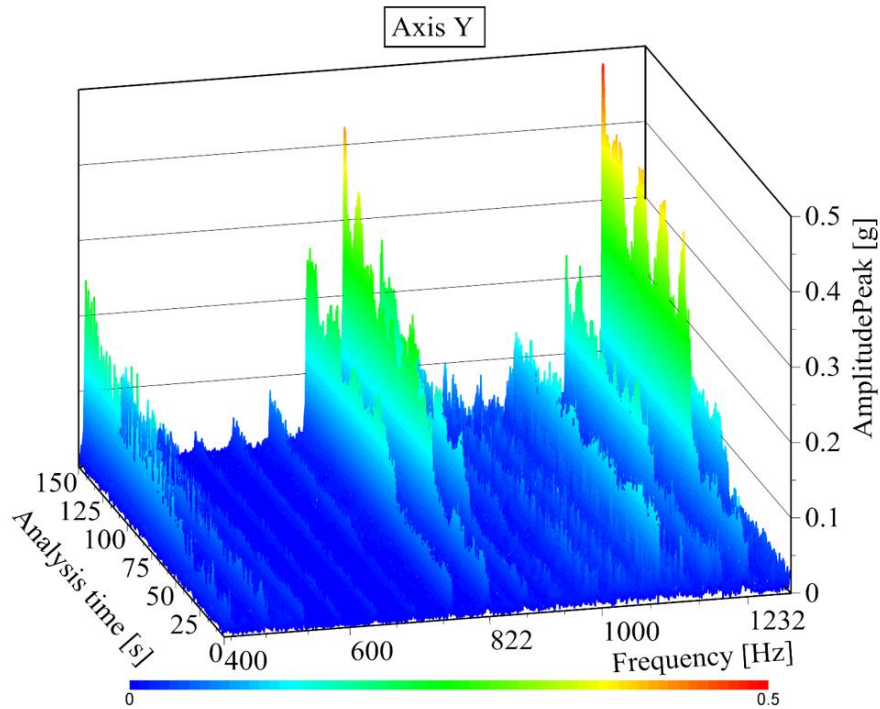


Figure 5. Waterfall analysis showed only in the range of 400 to 1300 Hz

Analyzing the waterfall chart, it is possible to identify the 410 Hz, 822 Hz and 1232 Hz as rising frequencies during the test. The 822 Hz and 1232 Hz can be characterized as second and third harmonics of the fundamental frequency, 410 Hz. This fundamental frequency matches the value reached with the Eq. 1 for the inner race frequency and, due to the rising of amplitude, can be characterized as the fault frequency. The rising phenomena can be more perceptible on Figure 6.

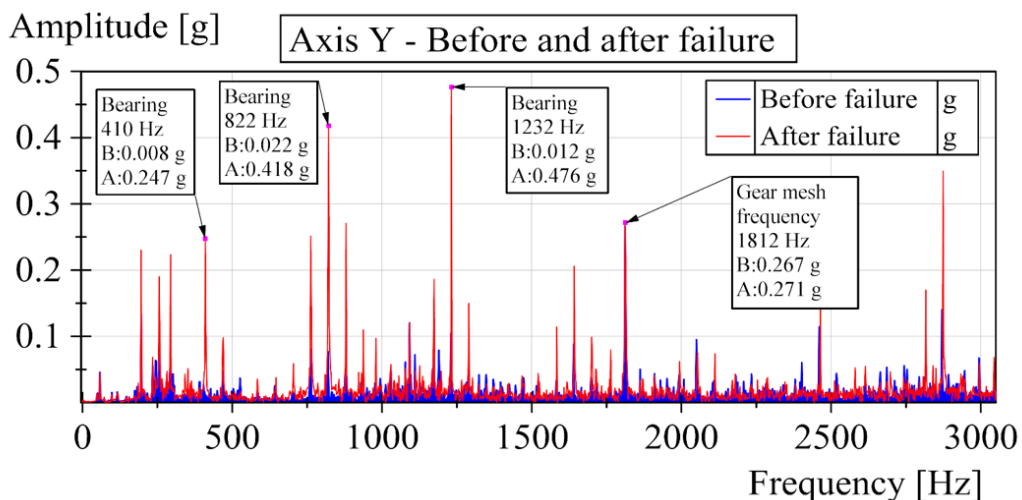


Figure 6. FFT analysis from the signal of the accelerometer mounted on the Y axis before and after failure

The 2D view in Figure 6, before and after the occurrence of the failure clarifies the identification of the rising fault frequency as 410 Hz. The rise of the amplitude reflects the change of state and occurrence of the failure, once the vibration of the bearing inner race is now amplified by the material removal from the surface. Although the Figure 6 shows only the Y-axis, these phenomena were perceived for X and Z orientation axes as well. The frequency 1812 Hz observed refer to the gear mesh due to rotation of the shaft and to the number of teeth present on the gear.

In order to summarize the developed method, Figure 7 presented below shows the diagram process applied on this study.

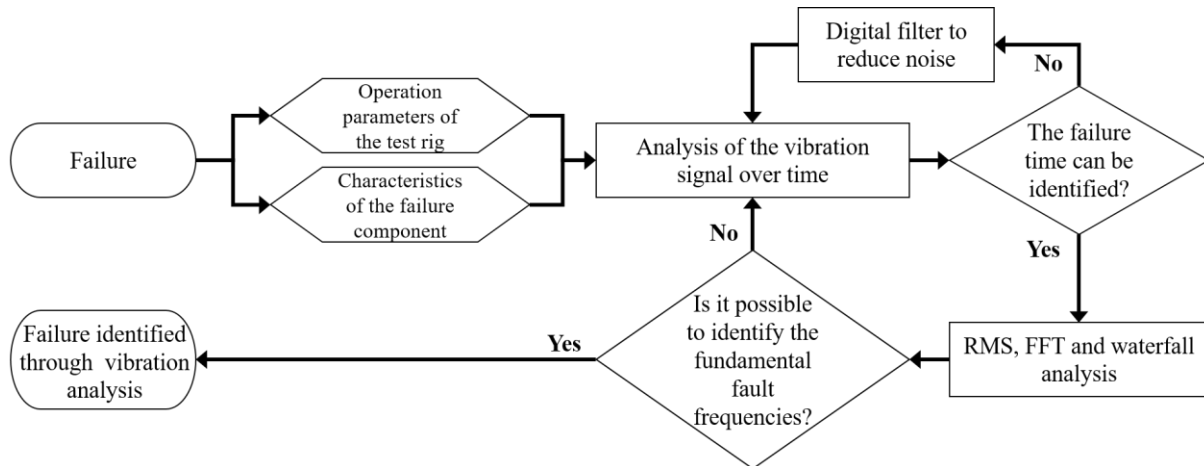


Figure 7. Analysis diagram

#### 4. CONCLUSIONS

With the RMS analysis, it was possible to identify the Y-axis as the direction that presented more increase of vibration amplitude. The values obtained from the equations to identify the bearing frequencies were essential to perform the correlation between the physic phenomena with the acquired data. From the FFT of the vibration signal it was possible to clearly identify the amplitude rising of the fault frequency from the inner race of the bearing as 410 Hz, according to the presented theory.

The waterfall analysis favored the visualization of the signals at the beginning of the failure and their behavior over time. Based on this, the developed method can be inserted on the online monitoring for the prediction of the early stages of fault, making possible the interruption of the test before the failure turns into catastrophic.

It is expected that this method can allow the identification of the exact fault component, such as gears or other bearings in the test rig, as well as the position of the fault, for example inner race or spheres of the bearings, without visual inspection. In the continuation of this study, the developed method will be investigated for others machine elements and it will be expanded to other failure modes. The development presented proved itself reliable for failure monitoring and can be effectively used for predictive maintenance of mechanical machinery.

#### 5. ACKNOWLEDGEMENTS

The authors gratefully acknowledge the support of the Programa Voluntário de Iniciação Científica do ITA (PIVIC-ITA) and of the Competence Center in Manufacturing of the Aeronautics Institute of Technology (CCM-ITA), where the research was conducted.

#### 6. REFERENCES

- Aslantas, K.; Tasgetiren, S.; Yalcin, Y., 2004, "Austempering retards pitting failure in ductile iron spur gears." Engineering Failure Analysis, vol. 11, p. 935-941.
- Brito, J. N., Monteiro, P. C, Christoforo, A. L., 2011, "Estudo de falhas em rolamentos provenientes de tensões e correntes parasitas utilizando sensor Shaft Probe", Vértices Magazine, V. 13, n 3, p 143-155, Rio de Janeiro, set./dez.
- Campanha, M. V, 2008, "Estudo sobre a vida útil de rolamentos fixos de uma carreira de esferas", Thesis, Escola Politécnica da Universidade de São Paulo – USP, São Paulo.
- Chiu, Y. P, Tallian, T. E., Mccool, J. I., 1971, "An engineering model of spalling fatigue failure in rolling contact: I – The subsurface model", Journal Wear, Vol. 17, pp. 433-446.

- Dybala, J., 2018, "Diagnosing of rolling-element bearings using amplitude level-based decomposition of machine vibration signal", *Journal Measurement*, Vol. 126, pp. 143-155.
- FZG, Description of the pitting test, Institute for Machine Elements – Gear Research Center, 1992.
- Graney, B. P., Starry, K., 2012, "Rolling Element Bearing Analysis", *Materials Evaluation*, Vol 70, No. 1, pp 78-85.
- Hoang, D. T, Kang, H. J., 2018, "Rolling element bearing fault diagnosis using convolutional neural network and vibration image", *Cognitive Systems Research*, 09 Aug. 2018 <<https://doi.org/10.1016/j.cogsys.2018.03.002>>
- Kotu, V., Deshpand, B., 2015 "Predictive Analytics and Data Mining: Concepts and Practice with RapidMiner", Ed. Morgan Kaufmann, Waltham, USA.
- Liu, R., Yang, B., Zio, E., Chen, X., 2018, "Artificial intelligence for fault diagnosis of rotating machinery: a review", *Journal of Mechanical Systems and Signal Processing*, Vol. 108, pp. 33-47.
- Mohammed, O. D., Rantatalo, M., Aindapää, J.O., Kumar, U., 2013, "Vibration signal analysis for gear fault diagnosis with various crack progressions scenarios", *Journal of Mechanical Systems and Signal Processing*, Vol. 41, pp 176-195.
- NKE Bearings, 2012, General Catalogue, NKE AUSTRIA GmbH.
- Wu, S., Zuo, M., Parey, A. 2008, "Simulation of spur gear dynamics and estimation of fault growth", *Journal of Sound and Vibration*, Vol. 317, pp. 608–624.

## **7. RESPONSIBILITY NOTICE**

The authors are the only responsible for the printed material included in this paper.